

# Direct electron acceleration by chirped laser pulse in a cylindrical plasma channel\*

Yong-Nan Hu(胡永南)<sup>1</sup>, Li-Hong Cheng(成丽红)<sup>2</sup>, Zheng-Wei Yao(姚征伟)<sup>1</sup>,  
Xiao-Bo Zhang(张小波)<sup>1</sup>, Ai-Xia Zhang(张爱霞)<sup>1</sup>, and Ju-Kui Xue(薛具奎)<sup>1,†</sup>

<sup>1</sup>College of Physics and Electronics Engineering, Northwest Normal University, Lanzhou 730070, China

<sup>2</sup>School of Science, Guizhou University of Engineering Science, Bijie 551700, China

(Received 4 December 2019; revised manuscript received 15 May 2020; accepted manuscript online 19 May 2020)

We study the dynamics of single electron in an inhomogeneous cylindrical plasma channel during the direct acceleration by linearly polarized chirped laser pulse. By adjusting the parameters of the chirped laser pulse and the plasma channel, we obtain the energy gain, trajectory, dephasing rate and unstable threshold of electron oscillation in the channel. The influences of the chirped factor and inhomogeneous plasma density distribution on the electron dynamics are discussed in depth. We find that the nonlinearly chirped laser pulse and the inhomogeneous plasma channel have strong coupled influence on the electron dynamics. The electron energy gain can be enhanced, the instability threshold of the electron oscillation can be lowered, and the acceleration length can be shortened by chirped laser, while the inhomogeneity of the plasma channel can reduce the amplitude of the chirped laser.

**Keywords:** chirped laser pulse, plasma channel, laser-plasma interaction, electron acceleration

**PACS:** 41.75.Jv, 52.38.Kd, 52.27.Ny, 52.38.Hb

**DOI:** [10.1088/1674-1056/ab943d](https://doi.org/10.1088/1674-1056/ab943d)

## 1. Introduction

Interaction between laser and plasmas can produce many physical phenomena such as laser self-guidance, harmonic excitation, wakefields generation, and electron acceleration.<sup>[1–8]</sup> Using ultra-intense laser pulse and plasma interaction to accelerate electrons has more obvious advantages than the conventional accelerators. Particularly, low-density plasmas have a conspicuous characteristic to obtain relativistic energetic electrons when a high-intensity laser beam is used, this feature has been demonstrated experimentally. Based on the study of the interaction between laser and plasma, many acceleration methods for obtaining high-energy electrons have been proposed. For example, direct laser acceleration (DLA), laser wake-field acceleration (LWFA) and plasma beat wave acceleration (PBWA).<sup>[9–22]</sup> These acceleration schemes make it possible to develop miniature, low-cost and table top particle accelerators. However, LWFA and PBWA schemes have high requirements for lasers, which is not conducive to reducing the cost of accelerators.<sup>[23,24]</sup> The disadvantage of the LWFA and PBWA schemes can be supplemented by the direct laser acceleration mechanism.

Direct laser acceleration is a kind of acceleration by binding electrons in the laser acceleration electric field under the combined action of the pondermotive force of the intense laser field and the strong electromagnetic field generated in the plasma. In the direct laser acceleration mechanism, the elec-

tron can be accelerated directly by the electric field of the laser, in which the acceleration gradient is linear with the laser amplitude. This linear relationship is the most obvious advantage of direct laser acceleration, which can effectively improve the acceleration efficiency. The direct laser acceleration may reduce the dependence of laser intensity greatly.<sup>[25]</sup> Although electrons can gain higher energy in the direct laser acceleration process, it is still limited by the Lawson–Woodward theorem and the final net energy gain of electrons is relatively small. The inverse Cherenkov acceleration mechanism was proposed to overcome the limitation of the Lawson–Woodward theorem and obtain the electrons of MeV energy.<sup>[26,27]</sup> However, when the intensity of laser exceeds a certain value, the neutral gas will be ionized by laser pulse and produce plasma, resulting in the failure of the inverse Cherenkov acceleration mechanism. Therefore, laser is one of the most important problems in particle acceleration. In recent years, chirped laser, which has been a hot issue, has a very promising application prospect in this field.

Along with the development of laser technology,<sup>[28–32]</sup> the chirped pulse amplification technology was proposed.<sup>[24]</sup> Then, the ultra-intense laser with the peak power of TW to PW was obtained on the experimental platform, and the amplification saturation effect and component loss caused by the rapid increase of laser intensity can be avoided effectively. The recent research on magnetized plasma shows that the peak

\*Project supported by the National Natural Science Foundation of China (Grant Nos. 11865014, 11765017, 11764039, 11475027, 11274255, and 11305132), the Natural Science Foundation of Gansu Province of China (Grant No. 17JR5RA076), the Scientific Research Project of Gansu Higher Education of China (Grant No. 2016A-005), the Natural Science Foundation of Education Department of Guizhou Province of China (Grant No. Qianjiaohe-KY-[2017]301), and the Science and Technology Project of Guizhou Province of China (Grant No. Qiankehe-LH-[2017]7008).

†Corresponding author. E-mail: [xuejk@nwnu.edu.cn](mailto:xuejk@nwnu.edu.cn)

power of laser can be realized 10 PW directly.<sup>[33]</sup> In recent years, great achievements have been made in the direct acceleration of electrons by chirped laser pulses.<sup>[7,34–37]</sup> It has been proved that chirped laser pulses can increase the energy of electrons by several hundreds of MeV on the basis of accelerating electrons by non-chirped laser pulses.<sup>[38]</sup> This is due to the chirped laser that breaks the distribution of the laser envelope and changes the acceleration phase of the laser by modulation of the frequency of the laser pulse. Furthermore, a method of using an external magnetic field is proposed, which significantly improves the efficiency of the chirped laser to accelerate the electron.<sup>[39]</sup> Using the chirped laser pulse in vacuum, dozens of GeV energetic electrons can be obtained.<sup>[38]</sup> However, laser can be easily scattered in vacuum. This characteristic of laser can be solved exactly in plasma. Especially, the self-focusing characteristics of laser in plasma make it possible for laser to keep the original radius and intensity transmission for a long distance. In order to guide laser more effectively over long distances, a method of guiding laser in pre-plasma channel has been proposed. It shows that when the energy of the electron increases, the electron appears to be unstable in the pre-plasma channel.<sup>[40,41]</sup> This instability exists a threshold. The threshold can be altered by changing the polarization angle of the laser pulse,<sup>[42]</sup> and it can increase the maximum energy of electrons.<sup>[40,43–48]</sup> Therefore, the direct laser acceleration of electrons in under-dense density plasma channel has attracted much attention. However, the coupling characteristics between chirped laser pulse and plasma channel and its effect on electron acceleration are still unclear.

In this work, the dynamics of single electron in homogeneous and inhomogeneous cylindrical plasma channels during the direct acceleration of linearly polarized chirped laser pulse are studied. The instability threshold of electron oscillation and the variation of electron energy with different types of chirped lasers and plasma parameters are given. In addition, the effects of different chirped laser pulse and plasma channel on the dephasing rate and trajectory of electron are also studied. The chirped laser and plasma channel have strong coupling effect on electron dynamics. The development of instability with chirped laser is faster and stronger than that for the non-chirped case. The accelerating length is shortened and the instability threshold is lowered by the chirped laser. The inhomogeneous density of plasma can reduce the threshold of the chirped laser amplitude significantly. That is, electrons can obtain higher energy gain from chirped laser pulse with lower instability threshold and larger instability oscillation region. We propose a method to further reduce the dependence of electron acceleration on laser intensity by changing chirped pulse frequency and inhomogeneous plasma channel.

## 2. The model and theoretical analysis

In order to examine the mechanism responsible for the enhancement of electron acceleration, we mainly focus on the single electron motion. The single electron is directly accelerated by a linearly polarized chirped segmented laser pulse with a phase velocity  $v_p$  in inhomogeneous cylindrical plasma channel with plasma density distribution  $n(r) = n_0[1 + m(r)]$ , where  $n_0$  is the equivalent charge density at the axis of plasma channel,  $m(r)$  is the inhomogeneous density distribution of plasma channel. Inhomogeneous density distribution can be generated by launching laser pulses transversely into gas jets or by transmitting pre-pulses and a proper delayed main pulses when using solid targets. In particular, linearly and parabolic inhomogeneous density distribution have been successfully and widely used in theoretical research, such as the excitation of THz radiation,<sup>[8,49]</sup> wake-field generation<sup>[50]</sup> and nonlinearly phenomena of relativistic and ponderomotive self-focusing in a plasma channel.<sup>[51]</sup>

Pulse dispersion occurs when laser beam is propagated in plasma channel. In general, the laser phase velocity will exceed the speed of light. The phase velocity of laser in vacuum is equal to the speed of light. Two independent dispersion sources must be considered when the laser pulse is dispersing through the plasma: the dispersion caused by the existence of plasma itself and the dispersion caused by the plasma channel under the action of intense laser pulse. The dispersion caused by the plasma itself will lead to the broadening of the laser pulse plasma. The dispersion of plasma channel under the action of intense laser pulse is limited by laser amplitude and channel size. The effect of laser phase velocity on the acceleration process is mainly reflected in the longitudinal momentum of the electron. According to the critical amplitude condition  $a_0 \approx \sqrt{2c/(v_p - c)}$ ,<sup>[52]</sup> the critical amplitude of laser pulse is  $a_0 = 20$ . In this work, the maximum amplitude of laser pulse is  $a_0 = 15$ . Under the critical amplitude condition, the effect of phase velocity on electronic dynamics is similar to that of vacuum. Therefore, the laser phase velocity in the preplasma channel is approximately the phase velocity in vacuum,<sup>[53]</sup> so we use the phase velocity of laser pulse in the pre-plasma channel  $v_p$  approximately equal to the speed of light  $c$  in vacuum. We choose a three-dimensional Cartesian system of coordinates  $(x, y, z)$ . The electromagnetic wave propagates in the positive  $z$  direction directed along the axis of the plasma channel. Here  $x$  and  $y$  are directed cross the channel, respectively. There is a transverse electrostatic field caused by charge separation in the plasma channel, it can be express as

$$E_c^x = e_x \omega_{p0}^2 m_e \frac{1}{|e|} \left[ \frac{1}{2}x + \frac{x \int m(r) r dr}{x^2 + y^2} \right], \quad (1)$$

$$E_c^y = e_y \omega_{p0}^2 m_e \frac{1}{|e|} \left[ \frac{1}{2}y + \frac{y \int m(r) r dr}{x^2 + y^2} \right], \quad (2)$$

where  $e_x$  and  $e_y$  are unit vectors,  $\omega_{p0} = \sqrt{4\pi n_0 |e|^2 / m_e}$  is the plasma frequency,  $m_e$  and  $e$  are the rest mass and charge of electron. In addition to the electrostatic field of the plasma channel, the electron is also affected by the electric field and magnetic field of the wave. The wave field can be described by  $\mathbf{E}_w^y = -\frac{m_e c}{|e|} \frac{\partial \mathbf{a}}{\partial t}$  and  $\mathbf{B}_w^x = \frac{m_e c^2}{|e|} \nabla \times \mathbf{a}$ , where superscripts  $x$  and  $y$  indicate the direction of wave field,  $\mathbf{a} = a(\xi) e_y$  is the wave field in terms of a dimensionless vector potential for linearly polarized chirped light,  $a(\xi)$  is a sinusoidal function with a slowly varying envelope.<sup>[41]</sup>

We use a segmented chirped laser pulse<sup>[42]</sup>

$$a(\xi) = \begin{cases} a_0 \exp\left[-\frac{(\xi - \xi_0)^2}{2\sigma^2}\right] \sin[\Omega(\xi)\xi], & \xi < \xi_0; \\ a_0 \sin[\Omega(\xi_0)\xi], & \xi \geq \xi_0, \end{cases} \quad (3)$$

where  $a_0$  is the incoming wave amplitude,  $\xi = \omega_0(t - z/c)$  is

a single dimensionless phase variable;  $\sigma$  is the pulse width,  $\xi_0$  is the length of the chirped laser pulse half-envelope. We set  $\sigma = 20$  and  $\xi_0 = 50$ .  $\Omega(\xi) = \omega(\xi)/\omega_0$  is the dimensionless laser frequency which varies with  $\xi$ . Here, it represents the chirped functions.

The segmented laser pulse<sup>[42]</sup> has the following advantages for electron acceleration. The first section of the laser pulse accelerates the electron firstly, while the second segment of the laser keeps the energy of the electron. Secondly, the electron is accelerated on the rising edge of the laser, but the most prominent position of the acceleration effect is near the peak of the laser pulse and extends to the second section of laser pulse. Finally, the synchronous interaction between the low frequency part of the laser magnetic field and the electron is beneficial not only to the acceleration of the electron but also to the energy holding of the accelerated electron.

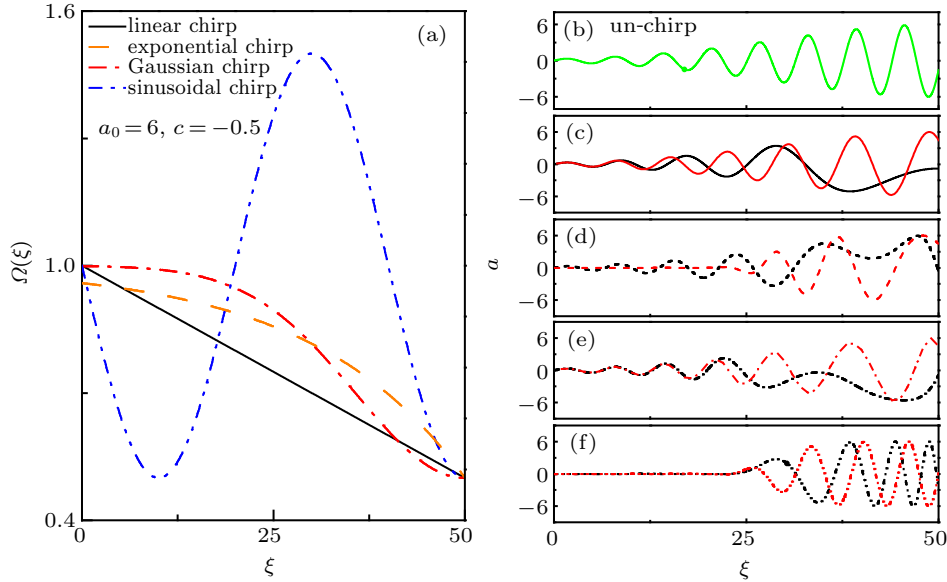


**Fig. 1.** Variation of laser frequency (a) and ramp-up of the laser amplitude against  $\xi$  for un-chirped case (b) and four chirped functions (c)–(f). In (c)–(f), the red curve is with  $c = -0.2$ , the black curve is with  $c = -0.5$ . The curve for each chirped function is shown in the figure.

In this study, we choose four chirped frequency functions, including linearly chirped function ( $\Omega(\xi) = 1 + c\xi/\xi_0$ ), Gaussian chirped function ( $\Omega(\xi) = 1 + c \exp[-(\xi - \xi_0)^2/\sigma^2]$ ), sinusoidal chirped function ( $\Omega(\xi) = 1 + c \sin(\xi\pi/\sigma)$ ) and exponential chirped function ( $\Omega(\xi) = 1 + c \exp(\xi/\sigma)/\exp(\xi_0/\sigma)$ ), where  $c$  is the normalized chirped parameter. Generation of high intensity laser pulses with a considerable chirp is possible with current technology and the chirped laser pulses have been experimentally implemented.<sup>[54–56]</sup> A linearly frequency chirp can be generated using two fiber Bragg gratings and a mode-locked fiber laser,<sup>[57,58]</sup> the chirp frequency can be controlled by adjusting the parameters of the optical system. The chirp frequency of exponential type is also realized,<sup>[59]</sup> and the sinusoidal chirp frequency across a molecular transition can be produced by applying modulation to the injection current, which use a quan-

tum cascade laser (QCL) or any other semiconductor laser as a source.<sup>[60]</sup> It is expected that the Gaussian chirped laser pulse can be realized with the development of laser technology in experiment in the near future. In recent years, these types of chirped pulses have been widely used in the field of laser-plasma interaction research.

At present, relative chirp of a few percents can be generated with solid-state laser systems.<sup>[61,62]</sup> High intensity laser pulses with a maximum chirp rate of about 10 percent can be obtained by the low-cycle systems or intense femtosecond laser pulses pass through the plasma channel.<sup>[63]</sup> Experimentally, the frequency of chirp generated by a free electron laser can be adjusted to 10 percent.<sup>[64]</sup> The larger chirp parameters are selected to verify the threshold conditions between the laser amplitude, channel density and the chirp parameters (Eq. (23)), and to explore the relationship between energy gain

of electron with the increase of the chirp parameters in the process of accelerating. The results show that the frequency shift of ultrashort-short laser pulses occurs when they collide with the ionization front two opposite directions, and the frequency shift efficiency can reach up to 75 percent.<sup>[55]</sup> This provides theoretical support for the realization of larger chirped laser pulses in the future, which is expected to be realized in the near future. In this work, we consider the negative chirped case, i.e.,  $c < 0$ . In order to study the role of chirped pulses in the process of electron acceleration, the evolution of the amplitude and frequency of different types of chirped laser pulses against  $\xi$  are illustrated in Fig. 1. The effect of four chirped frequency on ramp-up of the laser amplitude and laser asymmetry is shown in Figs. 1(c)–1(f). The frequency of the chirped laser pulse varies with the propagation of laser, which makes the laser envelope distribution asymmetric, and then enhances the intensity gradient and the pondermotive force of the laser. In addition, the low frequency duration of laser pulse is enhanced, which increases the synchronous interaction between the electron and the laser pulse. The larger the chirp parameter  $|c|$  is, the stronger the asymmetry of the laser does. The nonlinearly chirped laser pulse has stronger asymmetry and longer duration of low frequency than that of the linearly chirped pulse. Therefore we predict that the electron can obtain more energy from the chirped laser pulse. The electron can stay in the accelerating phase with laser pulse for a long time when chirped pulse laser is used, which can result in higher energy gain of electron. The numerical simulation confirm this prediction.

Under the action of magnetic fields ( $B_w^x$ ) and electric field ( $E_c^x$ ,  $E_c^y$  and  $E_w^y$ ), the electron dynamics is governed by

$$\frac{d\mathbf{r}}{dt} = \frac{\mathbf{p}}{\gamma m_e}, \quad (4)$$

$$\frac{d\mathbf{p}}{dt} = -|e|\mathbf{E} - \frac{|e|}{\gamma m_e c} [\mathbf{p} \times \mathbf{B}], \quad (5)$$

where  $\mathbf{r}$  is the electron position,  $t$  is the time in the plasma channel frame of reference,  $\mathbf{p}$  is the electron momentum;  $\gamma = \sqrt{1 + (p_x/m_e c)^2 + (p_y/m_e c)^2 + (p_z/m_e c)^2}$  is the relativistic factor. Using the following normalized parameters

$$\omega_{p0} \sim \frac{\omega_{p0}}{\omega_0}, \quad \mathbf{r} \sim \frac{\mathbf{r}}{c\omega_0^{-1}}, \quad t \sim \frac{t}{\omega_0^{-1}}, \quad \mathbf{p} \sim \frac{\mathbf{p}}{m_e c},$$

$$\mathbf{E} \sim \mathbf{E} \frac{e}{m_e \omega_0 c}, \quad \mathbf{B} \sim \mathbf{B} \frac{e}{m_e \omega_0 c}, \quad \mathbf{a} = \frac{|e|}{m_e c^2} \mathbf{A}. \quad (6)$$

Equations (4) and (5) can be written as

$$\frac{dp_x}{d\tau} = -\omega_{p0}^2 \gamma \left[ \frac{1}{2} x + \frac{x \int m(r) r dr}{x^2 + y^2} \right], \quad (7)$$

$$\frac{dp_y}{d\tau} = -\omega_{p0}^2 \gamma \left[ \frac{1}{2} y + \frac{y \int m(r) r dr}{x^2 + y^2} \right] + \frac{da}{d\tau}, \quad (8)$$

$$\frac{dp_z}{d\tau} = p_y \frac{da}{d\tau}, \quad (9)$$

$$\frac{dx}{d\tau} = p_x, \quad \frac{dy}{d\tau} = p_y, \quad \frac{dz}{d\tau} = p_z, \quad (10)$$

$$\frac{d\xi}{d\tau} = \gamma - p_z, \quad (11)$$

$$\gamma = \sqrt{1 + p_x^2 + p_y^2 + p_z^2}, \quad (12)$$

where  $n_0/n_c = \omega_{p0}^2$  ( $n_c$  is critical density of plasma),  $\tau$  is dimensionless time, which is used to replace the  $t$ . The relation between them is  $d\tau/dt = 1/\gamma$ .

From Eqs. (7)–(12), we obtain the following motion integral for electron:

$$I = \gamma - p_z + \frac{1}{4} \omega_{p0}^2 (x^2 + y^2) + \frac{1}{2} \omega_{p0}^2 \left[ \int x \frac{\int m(r) r dr}{x^2 + y^2} dx + \int y \frac{\int m(r) r dr}{x^2 + y^2} dy \right], \quad (13)$$

where  $r = \sqrt{x^2 + y^2}$ ,  $I$  is a constant and is determined by the initial conditions of the electron. We can set  $I = 1$  when initially the electron is stationary and the off-axis displacement of electron is very small. From Eq. (13), we can reach a relationship  $\gamma - p_z = 1 - s_1(x, y) - s_2(x, y) - s_3(x, y)$ , where  $\gamma - p_z$  is the dephasing rate, which denotes whether the electron can stay in a phase with the wave or not. The dephasing rate  $\gamma - p_z$  becomes small when the amplitude of oscillation of electron reaches the maximum amplitude  $r_{\max}$ .<sup>[40]</sup> Namely,  $\gamma - p_z \rightarrow 0$ , then the electron can obtain more energy from laser pulse, i.e., the result of  $\gamma/\gamma_{\text{vac}} > 1$ . We combine Eqs. (12) and (13), then the expression of  $p_z$  is

$$p_z = \frac{1}{2} \left\{ -[I - s_1(x, y) - s_2(x, y) - s_3(x, y)] + \frac{1 + p_x^2 + p_y^2}{[I - s_1(x, y) - s_2(x, y) - s_3(x, y)]^2} \right\}, \quad (14)$$

where  $s_1$ ,  $s_2$ , and  $s_3$  read

$$s_1(x, y) = \frac{1}{4} \omega_{p0}^2 (x^2 + y^2), \quad (15)$$

$$s_2(x, y) = \frac{1}{2} \omega_{p0}^2 \left[ \int x \frac{\int m(r) r dr}{x^2 + y^2} dx \right], \quad (16)$$

$$s_3(x, y) = \frac{1}{2} \omega_{p0}^2 \left[ \int y \frac{\int m(r) r dr}{x^2 + y^2} dy \right], \quad (17)$$

substituting Eq. (14) into Eq. (7)

$$\frac{d^2x}{d\xi^2} = -\frac{1}{2} \omega_{p0}^2 \left[ x + \frac{x \int m(r) r dr}{x^2 + y^2} \right] \times \left[ \frac{1}{2} + \frac{1 + p_x^2 + p_y^2}{2[I - s_1(x, y) - s_2(x, y) - s_3(x, y)]^2} \right], \quad (18)$$

holds under the condition that  $d/d\tau$  is replaced by  $d/d\xi$  ( $d\xi/d\tau = \gamma - p_z$ ), which results from the vector-potential described by  $\xi$ . Electron oscillates under the action of laser and plasma, the dominant force experienced by the electron is the force from the electric field of the wave. Even though the energy from the laser pulse is transferred to the transverse electron oscillations, the Lorentz force converts most of this energy into the longitudinal electron motion.<sup>[40]</sup> In under-dense



plasma channel  $\omega_{p0}^2 \ll 1$ , the approximate analytical solutions to Eqs. (4) and (5) is  $p_y \approx a$ . Applying  $a(\xi) = a_0 \sin[\Omega(\xi_0)\xi]$  for  $\xi > \xi_0$ , and setting  $l = 1$  (the initial off-axis displacement of the electron is small), equation (18) can be modified to the Mathieu equation

$$\frac{d^2x}{d\varphi^2} + [h - q \cos(2\varphi)] \left[ x + \frac{x \int m(r) r dr}{x^2 + y^2} \right] = 0, \quad (19)$$

where  $\varphi = \Omega(\xi_0)\xi$  and

$$h = \left( \frac{4}{a_0^2} + 1 \right) \frac{a_0^2 \omega_{p0}^2}{8\Omega^2(\xi_0)}, \quad q = \frac{a_0^2 \omega_{p0}^2}{8\Omega^2(\xi_0)}. \quad (20)$$

Equation (19) describes the stability of the electron oscillation in the plasma channel. Interestingly, the laser pulse and the inhomogeneous density of the plasma channel have coupled influence on the instability. We will discuss this separately in the following.

### 3. Uniform plasma channels

In this section, we consider the case of uniform plasma channel, i.e.,  $n(r) = n_0$ . Thus equation (19) can be written as

$$\frac{d^2x}{d\varphi^2} + [h - q \cos(2\varphi)] x = 0. \quad (21)$$

Equation (21) has a solution that grows exponentially  $x(\varphi) \propto \exp(\mu\varphi)$  with  $\mu$  being the growth rate determined by parameter  $h$  and  $q$ .<sup>[41]</sup> The electron dynamics are coupled to the relativistic factor in the  $xz$  plane and  $yz$  plane. The unstable oscillation of electron occurs (i.e.,  $\mu > 0$ ) when the  $h$  and  $q$  exceed a certain value. This instability can result in the electron energy enhancement and the electron oscillation along the  $x$  axis becomes unstable. We can approximately come to a conclusion of  $h$  and  $q$  when we consider the larger wave amplitude,

$$h \approx q. \quad (22)$$

The Mathieu equation is just related to the condition of  $h \approx q$ , where  $q = \frac{a_0^2 \omega_{p0}^2}{8\Omega^2(\xi_0)}$ , then we get a relation

$$a_0 \omega_{p0} = 2\sqrt{2}h\Omega(\xi_0). \quad (23)$$

To obtain the influence of chirped laser on the threshold of electron instability, we obtain the ranges of  $h$  and  $q$  from the intensity of laser and density of plasma and work out the unstable starting point with  $h = 0.48$  from the numerical solution of the Mathieu equation and the relation between parameters  $a$  and  $q$ .<sup>[41]</sup> Then, the unstable oscillation threshold of the electron can be obtained from Eq. (23) and the results are shown in Fig. 2. In Fig. 2, different curves represent the unstable threshold for different laser frequencies. As the laser frequency decreases, the corresponding parameters ( $a_0$ ,  $\omega_{p0}$ ) for occurring unstable oscillation of electron decreases, i.e., the threshold is reduced significantly. This indicates that the chirped laser

pulse, i.e., the variation of the laser frequency should have significant modification of the electron dynamics. In particular, when the chirp parameter is negative, the interaction time between the electron and the low frequency part of the laser magnetic field is enhanced, which provides favorable conditions for the electron to obtain energy in the laser. In addition, the intensity of the chirped laser pulse, the density of plasma channel, and the chirped function of the laser will play important roles on unstable oscillation of electrons. The chirped parameter modulation can greatly lower the threshold of the laser and plasma. We can select the corresponding chirped laser and chirp parameter to obtain higher energy electron on the basis of reducing the threshold of electron instability.

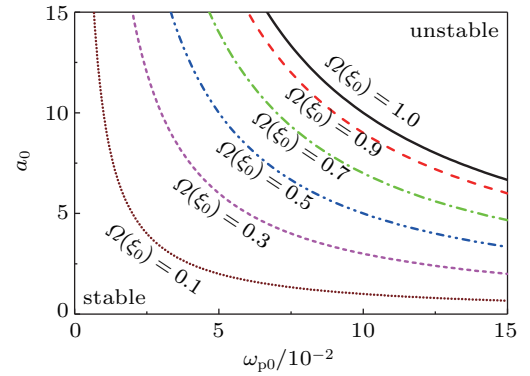
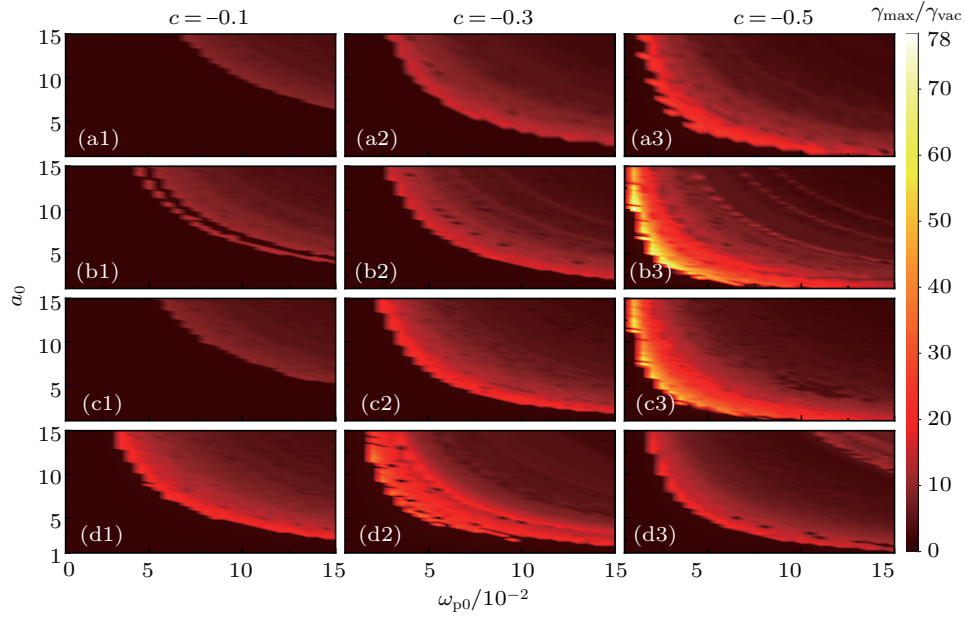


Fig. 2. The stability phase diagram of electron oscillation in  $(a_0, \omega_{p0})$  plane for different laser frequencies  $\Omega(\xi_0)$ .

To confirm the prediction shown in Fig. 2, we present in Fig. 3 the numerical results of electron dynamics based on numerical solution of Eqs. (7)–(12) with different intensity of laser pulse, density of plasma channel and chirped laser frequency function. In all numerical solutions, the initial conditions set as  $x(0) = y(0) = 0.05$  and  $p_x(0) = p_y(0) = p_z(0) = 0$ . Figure 3 shows  $\gamma_{\max}$  as functions of intensity of chirped laser pulse  $a_0$ , density of plasma channel  $\omega_{p0}$  and chirped laser frequency function  $\Omega(\xi)$ . The linearly (the first row of Fig. 3), exponential (the second row of Fig. 3), Gaussian (the third row of Fig. 3) and sinusoidal (the fourth row of Fig. 3) chirped lasers are used. For the un-chirped laser case, the maximum value of  $\gamma_{\max}/\gamma_{\text{vac}}$  is only 9.62. However, the maximum value of electron energy can reach up to 33.8 for linearly chirped laser (see Fig. 3(a3)), to 78.4 for exponential chirped laser (see Fig. 3(b3)), to 66.2 for Gaussian chirped laser (see Fig. 3(c3)), to 40.8 for sinusoidal chirped laser (see Fig. 3(d3)), respectively. Furthermore, we can easily see that the threshold of electron oscillation instability is reduced significantly with chirped laser, especially for exponential and Gaussian chirped lasers. This agrees with the results shown in Fig. 2. However, the difference in the threshold of electron instability is obvious for different chirped lasers with the same chirp parameter, which is caused by the different asymmetry of the chirped laser. This is consistent with the results shown in Fig. 1.



**Fig. 3.** Contour plot of  $\gamma_{\max}$  in  $(a_0, \omega_{p0})$  plane with different chirped laser pulses [linearly chirped laser pulse (the first row), exponential chirped laser pulse (the second row), Gaussian chirped laser pulse (the third row), and sinusoidal chirped laser pulse (the fourth row)]. Initially, the electron is at rest, but it is slightly displaced from the  $x$  and  $y$  axes of the plasma channel.

Compared to the results of the un-chirped laser pulse, the instability threshold can be lowered and the electron energy gain can be enhanced significantly with chirped laser pulse. The main physical mechanism can be understood as follows. The asymmetry of the laser can be changed by regulating the chirped factor (see Figs. 1(b)–1(f)). Moreover, the asymmetry of the laser enhances the laser intensity gradient and distorts the laser pondermotive force. Furthermore, the chirped laser field has a longer accelerating phase, which can be used to transform the electron injection position in the plasma channel. Meanwhile, it can increase the velocity of electron injection (due to the characteristics of segment laser, electron is accelerated at  $\xi > \xi_0$ ). For  $\xi > \xi_0$ , the laser frequency is also modulated by the chirped parameter. That is, the electron can get higher energy with shorter accelerating length under lower density of plasma channel. In general, on the one hand, the asymmetry of the chirped laser pulse improves the acceleration gradient of laser. On the other hand, the chirped frequency modulation enhances the synchronous interaction between the low frequency part of the laser magnetic field and electrons.

The dynamics of the electron shown in Fig. 3 can be further understood by the dephasing rate of the electron. As an example, we choose the case with Gaussian chirped laser pulse to analyze the effects of the chirped parameters on electron energy and electron dephasing rate, respectively. In Fig. 4, we consider the effects of chirped parameters on electron energy, dephasing rate and electron displacement in the direction of laser oscillation. With un-chirped laser ( $c = 0$  in Fig. 4), the electron is not accelerated ( $\gamma/\gamma_{\text{vac}} = 1$ ), while the dephasing rate is maximum ( $\gamma - p_z = 1$ ) and the electron keeps staying at  $x = 0$ . However, for chirped laser cases, the maximum value of electron energy can reach up to 3.575 GeV for Gaussian

chirped laser (see Fig. 4 with  $\omega_{p0} = 0.05$  and  $c = -0.4$ ), while the dephasing rate of electron (Fig. 4(b)) can stay near 0 for a longer time and the oscillating displacement of the electron in the  $y$  direction also tends to the maximum value, the maximum displacement of electron in the  $y$  direction reaches to 6.3 (see Fig. 4). Furthermore, for the Gaussian chirped laser pulse, the large the  $|c|$  is, the more slowly the dephasing rate  $\gamma - p_z$  changes, then the electron gains higher energy from the chirped laser pulse. Especially, the energy gain of the electron is the largest near the threshold of the instability oscillation.

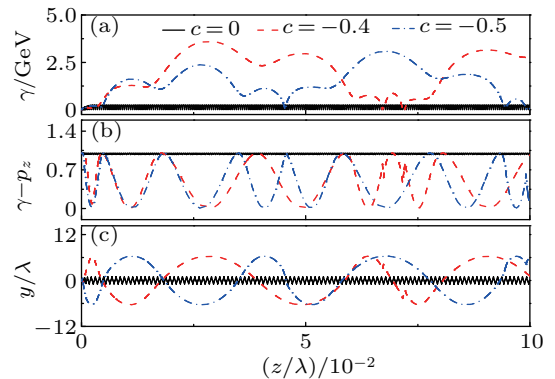


**Fig. 4.** Variation of  $\gamma/\gamma_{\text{vac}}$  (a), dephasing rate (b) and oscillation displacement in  $y$  direction (c) of electron against  $z/\lambda$  for different intensity of Gauss chirped laser under same plasma density ( $\omega_{p0} = 0.05$ ,  $a_0 = 6$ ).

Figure 5 shows the trajectories of the electron motion effected by the chirped pulse parameter. The electron can be accelerated to higher energy by the Gaussian chirped laser pulse and the oscillating displacement of the electron increases with the enhancement of the electron energy. Finally, it maintains a maximum oscillation displacement, the electron oscillates within this range. The electron will have a three-dimensional

motion, see Figs. 5(b)–5(d). We also find that the effective acceleration length of the electron is also shortened with the chirped laser pulse. Near the unstable threshold, the acceleration length is significantly shorter than that of other cases. This owes to the higher acceleration gradient of the chirped laser with stronger asymmetry.

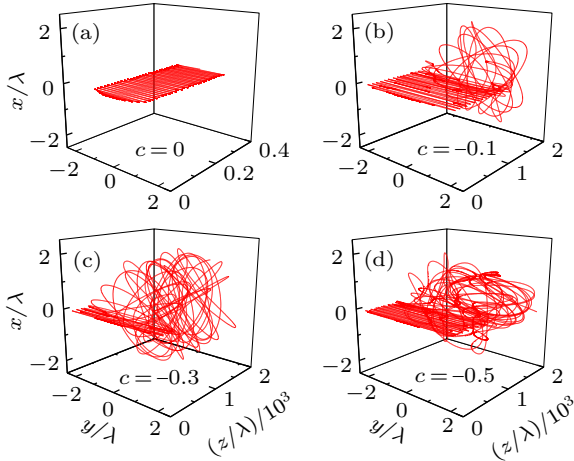


**Fig. 5.** The effect of Gaussian chirped laser pulse on the trajectory of single electron with different chirped pulse parameters, the amplitude of laser  $a_0 = 6$  and the density of plasma channel  $\omega_{p0} = 0.15$ .

In conclusion, the chirped factor has vital roles on unstable condition, maximum electron energy enhancement and the accelerating distance of electron. Especially in the aspect of electron energy gain, the chirped factor determines the asymmetry of the laser, and further determines the acceleration gradient of the laser. On the other hand, it enhances the low frequency duration of laser magnetic field. Compared with the un-chirped case, the electron energy gain increases approximately by one order of magnitude.

#### 4. Inhomogeneous plasma channels

When a laser beam propagates in the plasma channel, an equivalent charge separation field is generated when the ponderomotive force of laser expels out some electrons from the plasma along the transverse direction (the relative mass of the ions are relatively large and fixed). There are still a small number of electrons in the charge separation field, because the electrons in the channel are not completely emptied. Un-neutralized ion charges produce a reaction force that prevents the channel from being completely emptied. Thereby, it results in inhomogeneous plasma density distribution of the channel. Therefore, in the following analysis, the effect of inhomogeneous plasma density distribution in the channel on electron acceleration is considered.

We use two types of inhomogeneous plasma channel, i.e., linearly inhomogeneous plasma channel and parabolic inhomogeneous plasma channel, i.e.,  $m(r) = br$  and  $m(r) = br^2$ , where  $b$  is the inhomogeneous density parameter. We mainly

discuss the coupled influence of inhomogeneous plasma channel and chirped laser pulse on single electron dynamics.

The energy of electron is modulated by chirped laser and inhomogeneous plasma channel. As Fig. 6 shows, the maximum energy of electron is effected by the chirped parameter and inhomogeneous parameter. Because we assume that the plasma density increases outward from the axis of the cylindrical plasma channel, we set the initial density at the axis of the channel to be 0.05. The linearly (the first row in Fig. 6) and parabolic (the second row in Fig. 6) inhomogeneous plasma channel with the linearly (the first column in Fig. 6), exponential (the second column in Fig. 6), Gaussian (the third column in Fig. 6) and sinusoidal (the fourth column in Fig. 6) chirped laser pulses are used. Clearly, the electron dynamics is strongly modulated by the coupled effects of inhomogeneous plasma channel and the chirped laser pulse. The threshold of chirped amplitude for occurring the unstable electron oscillation is lowered significantly by the inhomogeneous plasma, especially for parabolic inhomogeneous plasma channel. Interestingly, the unstable region in  $(b, c)$  plane is highly modulated near the threshold line, the unstable oscillation of electron can take place only in some special region. This is particularly obvious with sinusoidal chirped laser pulse (Figs. 6(d) and 6(h)).

The underlying physics shown in Fig. 6 can be understood as follows. Equation (8) shows that the electron motion is a harmonic oscillation when the channel is uniform ( $m(r) = 0$ ), the oscillation frequency is  $\omega_{p0}\sqrt{\gamma/2}$ . The effect of laser on electron as an internal driving force, and the effect of plasma channel on electron as an external driving force.<sup>[53]</sup> The electron is accelerated under the synergistic effect of two driving forces.

For the inhomogeneous plasma, the inhomogeneous density distribution changes the magnitude of the external driving force, the external driving force of inhomogeneous plasma channel is greater than that of the homogeneous plasma channel. For linearly inhomogeneous plasma channel ( $m(r) = br$ ), if electron always moves along the axis of the channel, the acceleration effect will be consistent with the uniform channel case. Because of the existence of laser field, it is necessary for electrons to have a similar harmonic oscillation in the laser field. The farther the electron is from the axis of the channel, the greater the external driving force is, which also ensures that electrons do not escape the plasma channel during the acceleration process. For parabolic inhomogeneous plasma channel ( $m(r) = br^2$ ), the growth rate of the density gradient in the channel is greater than that in the linearly inhomogeneity case, i.e., parabolic inhomogeneous channel can provide stronger external driving force. The resonance effect occurs when the frequency of the internal driving force of the system is close to the frequency of the external driving force or the frequency doubling of the external driving force, and

the electron gets higher energy from the laser. Inhomogeneous density distribution increases the frequency of external driving force. However, with the increase of external driving force, the electron is limited in obtaining energy from laser. This is the

reason why the electron unstable oscillation is easy to occur in the parabolic inhomogeneous plasma channel whereas the energy gain is smaller than the linearly inhomogeneous plasma channel case.

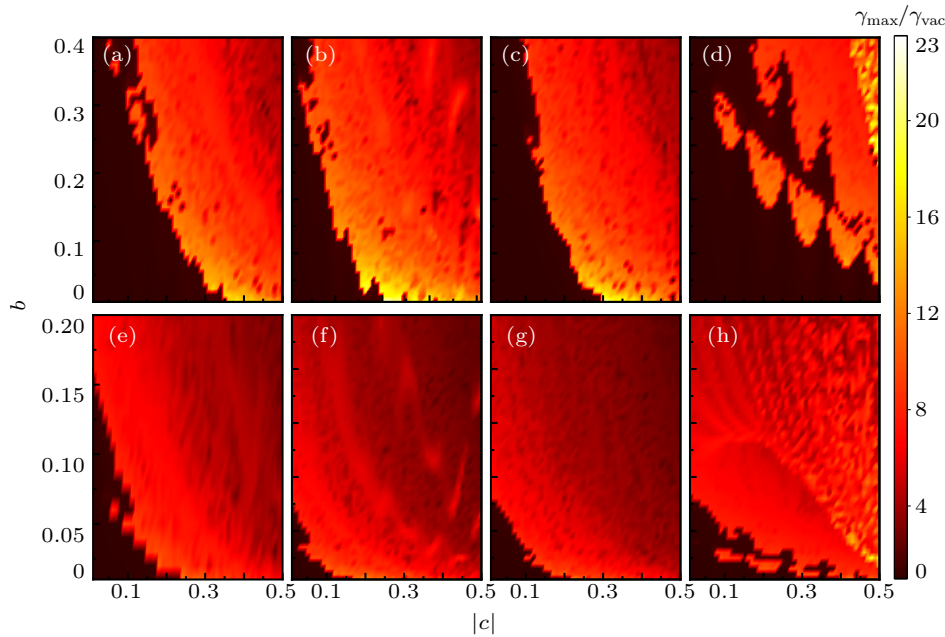


**Fig. 6.** The single electron is placed in linearly inhomogeneous plasma channel (the first row) and parabolic inhomogeneous plasma channel (the second row) respectively. It is irradiated by four types of chirped laser pulse (linearly chirped laser pulse in (a) and (e), Gaussian chirped laser pulse in (b) and (f), exponential chirped laser pulse in (c) and (g) and sinusoidal chirped laser pulse in (d) and (h)). The intensity of the laser pulse  $a_0 = 6$ , the plasma density at the axis of the channel is  $\omega_{p0} = 0.05$ , the density distribution for linearly inhomogeneous and parabolic inhomogeneous case are  $n(r) = 1 + br$  and  $n(r) = 1 + br^2$  (the  $r$  is radial direction). The maximum energy of electron is normalized by the maximum energy of electron in vacuum  $\gamma_{vac} = 1 + a_0^2/2$ .

## 5. Summary

We have analyzed the dynamics of the direct acceleration of electrons by chirped laser pulses in homogeneous and inhomogeneous cylindrical plasma channels. It is found that the occurrence of electron oscillation instability (i.e., electron acceleration) with chirped laser pulse is faster and stronger than that with un-chirped laser. Particularly, there is a strong coupled effect of the inhomogeneous plasma channel and the chirped laser pulse. The instability threshold, the acceleration length and the energy gain of electron acceleration in plasma channel can be controlled by adjusting the parameters of chirped laser pulse and distribution of inhomogeneous plasma density. We hope that our research will facilitate further experiments in this direction.

## Acknowledgment

The scientific contributions from other people or groups are acknowledged here. Financial supports are given in the footnote on the first page.

## References

[1] Sprangle P, Esarey E and Ting A 1990 *Phys. Rev. Lett.* **64** 2011  
 [2] Max C E, Arons J and Langdon A B 1974 *Phys. Rev. Lett.* **33** 209

[3] Bobin J L, Decroisette M, Meyer B and Vitel Y 1973 *Phys. Rev. Lett.* **30** 594  
 [4] Weng S M, Murakami M, Azechi H, Wang J W, Tasoko N, Chen M, Sheng Z M, Mulser P, Yu W and Shen B F 2014 *Phys. Plasmas* **21** 012705  
 [5] Esarey E, Ting A and Sprangle P 1990 *Phys. Rev. A* **42** 3526  
 [6] Faure J, Glinec Y, Santos J J, Ewald F, Rousseau J P, Kiselev S, Pukhov A, Hosokai T and Malka V 2005 *Phys. Rev. Lett.* **95** 205003  
 [7] Esarey E, Schroeder C B and Leemans W P 2009 *Rev. Mod. Phys.* **81** 1229  
 [8] Zhang Z, Chen Y, Cui S, He F, Chen M, Zhang Z, Yu J, Chen L, Sheng Z and Zhang J 2018 *Nat. Photon.* **12** 554  
 [9] Clayton C E, Joshi C, Darrow C and Umstadter D 1985 *Phys. Rev. Lett.* **54** 2343  
 [10] Zhao Q, Weng S M, Chen M, Zeng M, Hidding B, Jaroszynski D A, Assmann R and Sheng Z M 2019 *Plasma Phys. Control. Fusion* **61** 085015  
 [11] Clayton C E, Marsh K A, Dyson A, Everett M, Lal A, Leemans W P, Williams R and Joshi C 1993 *Phys. Rev. Lett.* **70** 37  
 [12] Krall J, Ting A, Esarey E and Sprangle P 1993 *Phys. Rev. E* **48** 2157  
 [13] Modena A, Najmudin Z, Dangor A E, Clayton C E, Marsh K A, Joshi C, Malka V, Darrow C B, Danson C, Neely D and Walsh F N 1995 *Nature* **377** 606  
 [14] Umstadter D, Dodd E and Kim J K 1996 *Phys. Rev. Lett.* **76** 2073  
 [15] Esarey E, Hubbard R F, Leemans W P, Ting A and Sprangle P 1997 *Phys. Rev. Lett.* **79** 2682  
 [16] Moore C I, Ting A, Mchaught S J, Qiu J, Burris H R and Sprangle P 1999 *Phys. Rev. Lett.* **82** 1688  
 [17] Wang X, Donovan M, Dyer G, Wang X M, Zgadaj R, Fazel N, Li Z Y, Yi S A, Zhang X, Henderson W, Chang Y Y, Korzekwa R, Tsai H E, Pai C H, Quevedo H, Dyer G, Gaul E, Martinez M, Bernstein A C, Borger T, Spinks M, Donovan M, Khudik V, Shvets G, Ditmire T and Downer M C 2013 *Nat. Commun.* **4** 1988



- [18] Leemans W P, Gonsalves A J, Mao H, Nakamura K, Benedetti C, Schroeder C B, Tóth C, Daniels J, Mittelberger D E and Bulanov S S 2014 *Phys. Rev. Lett.* **113** 245002
- [19] Rassou S, Bourdier A and Drouin M 2015 *Phys. Plasmas* **22** 073104
- [20] Pukhov A and Meyerter J 2002 *Appl. Phys. B* **74** 355
- [21] Pollock B B, Tsung F S, Albert F, Shaw J L, Clayton C E, Davidson A, Lemos N, Marsh K A, Pak A and Ralph J E 2015 *Phys. Rev. Lett.* **115** 055004
- [22] Lu W, Tzoufras M, Joshi C, Tsung F S, Mori W B, Vieira J, Fonseca R A and Silva L O 2007 *Phys. Rev. ST Accel. Beams* **10** 061301
- [23] Amiranoff F, Bernard D, Cros B, Jacquet F, Matthieussent G, Miné P, Mora P, Morillo J, Moulin F and Specka A E 1995 *Phys. Rev. Lett.* **74** 5220
- [24] Tajima T and Dawson J M 1979 *Phys. Rev. Lett.* **43** 267
- [25] Gahn C, Tsakiris G D, Pukhov A, Meyer-ter-Vehn J, Pretzler G, Thiroff P, Habs D and Witte K J 1999 *Phys. Rev. Lett.* **83** 4772
- [26] Dyakonov M I and Varshalovich D A 1971 *Phys. Lett.* **35** 277
- [27] Edighoffer J A, Kimura W D, Pantell R H, Piestrup M A and Wang D Y 1981 *Phys. Rev. A* **23** 1848
- [28] Koyama K, Hazama H, Saito N and Tanimoto M 2002 *Int. J. Appl. Electromagn. Mech.* **14** 263
- [29] Seres J, Seres E, Verhoef A J, Tempea G, Strelcić C, Wobruschek P, Yakovlev V, Scrinzi A, Spielmann C and Krausz F 2005 *Nature* **433** 596
- [30] Tatarakis M, Watts I, Beg F N, Clark E L, Dangor A E, Gopal A, Haines M G, Norreys P A, Wagner U and Wei M 2002 *Nature* **415** 280
- [31] Weng S, Zhao Q, Sheng Z, Yu W, Luan S, Chen M, Yu L, Murakami M, Mori W B and Zhang J 2017 *Optica* **4** 1086
- [32] Zheng X, Weng S, Zhang Z, Ma H, Chen M, McKenna P and Sheng Z 2019 *Opt. Express* **27** 19319
- [33] Liu M, Weng S M, Wang H C, Chen M, Zhao Q, Sheng Z M, He M Q, Li Y T and Zhang J 2018 *Phys. Plasmas* **25** 063103
- [34] Malka G, Lefebvre E and Miquel J L 1997 *Phys. Rev. Lett.* **78** 3314
- [35] Wu X Y, Wang P X and Kawata S 2012 *Appl. Phys. Lett.* **100** 221109
- [36] Gupta D N, Jang H J and Suk H 2009 *J. Appl. Phys.* **105** 106110
- [37] Hooker S M 2013 *Nature Photon.* **7** 775
- [38] Sohbatzadeh F, Mirzanejhad S and Ghasemi M 2006 *Phys. Plasmas* **13** 123108
- [39] Gupta D N and Suk H 2006 *Phys. Plasmas* **13** 013105
- [40] Arefiev A V, Khudik V N, Robinson A P L, Shvets G, Willingale L and Schollmeier M 2016 *Phys. Plasmas* **23** 056704
- [41] Arefiev A V, Breizman B N, Schollmeier M and Khudik V N 2012 *Phys. Rev. Lett.* **108** 145004
- [42] Arefiev A V, Khudik V N and Schollmeier M 2014 *Phys. Plasmas* **21** 033104
- [43] Raoa B S, Chakera J A, Naik P A, Kumar M and Gupta P D 2011 *Phys. Plasmas* **18** 093104
- [44] Zhang P, Hu Y, Li T, Cannan D, Yin X, Morandotti R, Chen Z G and Zhang X 2012 *Phys. Rev. Lett.* **109** 193901
- [45] Chelkowski S, Bandrauk A D, Corkum P B 1990 *Phys. Rev. Lett.* **65** 2355
- [46] Khachatryan A G, Van Goor F A and Boller K J 2004 *Phys. Rev. E* **70** 067601
- [47] Khachatryan A G, Van Goor F A, Verschuur J W and Boller K 2005 *Phys. Plasmas* **12** 062116
- [48] Pukhov A, Sheng Z M and Meyer-ter-Vehn J 1999 *Phys. Plasmas* **6** 2847
- [49] Sheng Z, Wu H, Li K and Zhang J 2004 *Phys. Rev. E* **69** 025401
- [50] Sheng Z, Mima K, Zhang J and Sanuki H 2005 *Phys. Rev. Lett.* **94** 095003
- [51] Layer B D, York A, Antonsen T M, Varma S, Chen Y, Leng Y and Milchberg H M 2007 *Phys. Rev. Lett.* **99** 035001
- [52] Robinson A P L, Arefiev A V and Khudik V N 2015 *Plasma Phys.* **22** 083114
- [53] Arefiev A V, Khudik V N, Robinson A P L, Shvets G and Willingale L 2016 *Phys. Plasmas* **23** 023111
- [54] Treacy E B 1968 *Phys. Lett. A* **28** 34
- [55] Dias J M, Stenz C, Lopes N, Badiche X, Blasco F, Dos Santos A, E Silva L O, Mysyrowicz A, Antonetti A and Mendonça J T 1997 *Phys. Rev. Lett.* **78** 4773
- [56] Pathak N, Zhidkov A, Hosokai T and Kodama R 2018 *Phys. Plasmas* **25** 013119
- [57] Zeitouny A, Stepanov S, Levinson O and Horowitz M 2005 *IEEE Photon. Technol. Lett.* **17** 660
- [58] Rao B S, Moorti A, Naik P A and Gupta P D 2013 *Phys. Rev. ST Accel. Beams* **16** 091301
- [59] Ojarand J and Annus P 2010 *Elektronika ir Elektrotehnika* **4** 73
- [60] Nikodem M, Weidmann D and Wysocki G 2012 *Appl. Phys. B* **109** 477
- [61] Faure J, Marquès J R, Malka V, Amiranoff F, Najmudin Z, Walton B, Rousseau J P, Ranc S, Solodov A and Mora P 2001 *Phys. Rev. E* **63** 065401
- [62] Brabec T and Krausz F 2000 *Rev. Mod. Phys.* **72** 545
- [63] Gordon D F, Hafizi B, Hubbard R F, Penano J R, Sprangle P and Ting A 2003 *Phys. Rev. Lett.* **90** 215001
- [64] Hajima R and Nagai R 2003 *Phys. Rev. Lett.* **91** 024801